Supplemental Materials

METHODS

Experimental Preparation

The procedures were approved by the Subcommittee on Research Animal Care of the Massachusetts General Hospital (Boston, Massachusetts). Twelve sheep (22.0±1.8 kg) were anesthetized, intubated and mechanically ventilated. All procedures were performed under strict aseptic conditions. Femoral artery, internal jugular vein and pulmonary artery catheters were inserted. A left-sided double-lumen endobronchial tube was placed through a tracheotomy, and used to produce lung surfactant depletion by alveolar saline lavage. Warm saline (~400 ml) was instilled in the left bronchus (pressure~30 cmH_2O) of initially supine sheep, followed by draining to gravity. After three aliquots, animals were turned prone for three additional aliquots, to homogenize lavage of ventral and dorsal regions. A regular endotracheal tube was then placed and double lung ventilation resumed.

Experimental Protocol

Animals were positioned supine in the PET scanner with the field of view immediately above the diaphragmatic dome. Mechanical ventilation was applied for four hours using: PEEP=10 cmH_2O, FiO_2=0.6, inspiratory-to-expiratory ratio 1:2, tidal volume adjusted to a plateau pressure of 30 cmH_2O and respiratory rate adjusted to normocapnia. Studies were sequential in each group. Transmission and ^{13}NN emission PET scans were performed at baseline and at the end of the four-hour mechanical ventilation period. ^{18}F-FDG-PET scans were acquired after the last set of ^{13}NN scans. Following baseline imaging, six sheep (LPS+ group) received a continuous 10 $ng.kg^{-1}.min^{-1}$ intravenous infusion of endotoxin (Escherichia coli O55:B5, List Biological Laboratories Inc, California) while six did not (LPS- group).

PET Imaging Protocol and Processing

The imaging methods and analysis have been previously described in detail (*1-4*). Briefly, the PET camera acquired 15 transverse cross-sectional slices of 6.5-mm thickness providing 3-dimensional information over a 9.7-cm-long field of view corresponding to ~70% of the total lung volume (*4*). Resulting reconstructed PET images consisted of an interpolated matrix of 128 × 128 × 15 voxels (2 x 2 mm in-plane) with a spatial resolution of approximately 6.5 mm defined as full width at half maximum. Three different types of scans were performed:

1) Transmission scans were obtained over 10 min prior to each emission scan to correct for attenuation in emission scans and to calculate the fraction of gas (F_{gas}) of different regions of interest (ROIs) from regional tissue density (F_{tissue}) as $F_{gas} = 1 - F_{tissue}$.

Because the transmission scan cannot differentiate tissue components with similar density, F_{tissue}, in the lungs, represents the fractional content of all components with unit density and therefore includes not only the contribution of parenchyma but also of blood, inflammatory infiltrates, and edema.

2) ^{13}NN emission scans with ^{13}NN-saline

These were performed for assessment of regional perfusion and shunt. The tracer ^{13}NN gas (~10-min half-life) was generated by a cyclotron and dissolved in degassed normal saline.

The imaging protocol started with a tracer-free lung. The ventilator was turned off at the beginning of the exhalation, and the airway pressure was maintained at a value equal to the mean airway pressure during ventilation. A 20–30 mL bolus of ^{13}NN-saline solution was then injected at a rate of 10 mL/s into the right internal jugular vein. Simultaneously, collection of a series of consecutive images was started. After an apnea period of 60 s, mechanical ventilation was restarted. The total imaging sequence lasted 4 min and consisted of 8 images of 2.5 s and 4

images of 10 s during apnea, and 6 images of 10 s and 4 images of 30 s during the washout phase.

Because of the low solubility of nitrogen in blood and tissues (partition coefficient water-to-air is 0.015 at 37°C), the pulmonary kinetics of infused ^{13}NN shows distinct characteristics in regions that are perfused and aerated and regions that are perfused but not aerated (*i.e.*, shunting units). In perfused and aerated regions, virtually all ^{13}NN diffuses into the alveolar airspace at first pass, and during apnea it accumulates in proportion to regional perfusion. In regions with shunting alveolar units, ^{13}NN kinetics during apnea show a peak of tracer concentration in the early PET frames, corresponding to arrival of the bolus of tracer with pulmonary blood flow, followed by a decrease towards a plateau. This decrease of activity reflects lack of retention of ^{13}NN in non-aerated units, and its magnitude is related to regional shunt. Perfusion and shunt fraction of the test and control lungs were calculated with a tracer kinetics model (*3-5*).

3) ^{18}F-FDG emission scans

These were obtained for quantification of regional ^{18}F-FDG kinetics. After ^{13}NN clearance, ^{18}F-FDG (5–10 mCi) was infused at a constant rate through the jugular catheter over 60 s and, simultaneous with the beginning of ^{18}F-FDG infusion, sequential PET frames (6 × 30 s, 7 × 60 s, 15 × 120 s, 1 × 300 s, 3 × 600 s) were acquired over 75 min. Blood samples were collected from pulmonary arterial blood at: 5’30’’, 9’30’’, 25’, 37’ and 42’30’’ to calibrate the input function (*6*). ^{18}F-FDG PET scans were acquired only after injury because of the 110-min half-life of ^{18}F-FDG.

The lung fields of the lavaged and non-lavaged lungs were delineated separately using both perfusion and gas fraction images.

Modeling of ^{18}F-FDG kinetics

After being transported into the cell by the same mechanism as glucose, ^{18}F-FDG is phosphorylated by hexokinase to ^{18}F-FDG-6-phosphate, which accumulates in proportion to the metabolic rate of the cell. ^{18}F-FDG uptake parameters were computed using a four-compartment model (*7*) developed as extension to Sokoloff's model (*8*) for pulmonary applications. The four-compartment model includes a blood and three tissue compartments (Supplemental Figure 1): k_1 represents the rate transfer of facilitated ^{18}F-FDG transport from blood into a tissular precursor compartment for ^{18}F-FDG phosphorylation (C_{ei}), per unit of lung volume; the rate constant k_2 quantifies tracer transport from the precursor compartment back into the blood, and k_3 is the rate transfer of ^{18}F-FDG from the precursor compartment to the metabolite compartment (C_m), that is the rate of ^{18}F-FDG phosphorylation to ^{18}F-FDG-6-phosphate, which is assumed to be proportional to hexokinase activity (*8*). An extravascular/noncellular tissue compartment (C_{ee}), representing a pool of ^{18}F-FDG that is not a direct substrate for phosphorylation, allows for discrimination between the distribution volume of ^{18}F-FDG that is (F_{ei}, intracellular) and that is not (F_{ee}, extravascular/noncellular) a precursor for phosphorylation. Rate constants k_5 and k_6 described the forward and backward transfer of ^{18}F-FDG between C_{ei} and C_{ee}.(*7*) The activity concentration in the region of interest (C_{ROI}) over time is given as:

$$C_{ROI}(t) = F_{blood} \cdot C_P(t) + C_{ei}(t) + C_{ee}(t) + C_m(t) \quad \text{Eq. 1}$$

Where $C_P(t)$ is the pulmonary arterial plasma ^{18}F-FDG concentration and F_{blood} is the ROI fractional blood volume derived from the ^{18}F-FDG kinetics.(*7*) From these, a measure of the net uptake rate of ^{18}F-FDG from plasma to tissue (Ki), as well as the distribution volume of the precursor compartment (F_{ei}) as a fraction of lung volume were computed:

$$Ki = k_1 \cdot k_3/(k_2+k_3) \quad \text{Eq. 2}$$

$$F_{ei} = k_1/(k_2+k_3) \quad \text{Eq. 3}$$

Thus, from equations 1 and 2

$$Ki = F_{ei} \cdot k_3 \quad \text{Eq. 4}$$

A tissue fraction, blood fraction and wet-to-dry ratio (w/d) corrected Ki (Ki_T) was calculated to account for the effects of changes in: i) regional lung density, by dividing Ki by the tissue fraction, after excluding the blood volume (F_{tissue}-F_{blood} = 1-F_{gas}-F_{blood}) and ii) wet-to-dry ratio, to account for increased regional density due to elevated lung water rather than lung tissue, for both lavaged and non-lavaged lungs. Thus, the normalized uptake rate (Ki_T) is proportional to tissue volume or an equivalent number of alveoli. Using a reference value for normal sheep lung wet-to-dry ratio ($w_N/d_N \sim 3.7$),(*9, 10*) we calculated:

$$Ki_T = Ki \cdot (w/d)/((F_{tissue}-F_{blood}) \cdot (w_N/d_N)) = Ki \cdot (w/d)/((1-F_{gas}-F_{blood}) \cdot (w_N/d_N)) \quad \text{Eq. 5}$$

Lung Cytokine Measurement

Regional lung expression of TNF-α, IL-1β, IL-6, IL-8, and IL-10 was measured using real-time RT-PCR (qRT-PCR). For each target gene, primers were selected using Primer3 software (http://www.broad.mit.edu/cgi-bin/primer/primer3.cgi/; (*11*)). The default parameters of the program were applied, except for the following: product size 100–150 bp; primer size 18–22 bp. Primers were selected using the following criteria (in order of importance, Supplemental Table 1): (1) forward and reverse primers were placed on two consecutive exons of the gene where possible, (2) no more than three Gs or Cs within the last five nucleotides in the 3′ termini of primers.

After lungs were harvested, lung tissue samples from ventral and dorsal regions of each lung were snap frozen in liquid nitrogen and stored at -80° C. Total RNA was extracted from ovine lung tissues using Tri reagent (Sigma, St. Louis, USA). 1 μg of RNA was converted to

cDNA using M-MLV reverse transcriptase (Promega Corporation, Madison, WI, USA) according to the manufacturer's instructions. Quantitative real-time PCR reactions were run in 20 μL containing 10 μL of SYBR green master mix, 1.25 μM each primer, and 6 μL of template cDNA, made up to 20 μL with deionized water. The cycling conditions for all genes were as follows: 15 minutes at 95°C, 40 cycles of 15 seconds at 95°C and 1 minute at 60°C, followed by a melt curve starting at 60°C rising to 95°C at 0.03°C per second. Copy numbers were determined from the Ct values of each sample. Final quantitation was performed by comparison with the internal standard, glyceraldehyde-3-phosphate dehydrogenase (GAPDH) housekeeping gene ($2^{-\Delta\Delta Ct}$).

Lung Histology and Wet-to-Dry Lung Ratios

After fixation, lung tissue samples were embedded in paraffin. Five-μm thick tissue samples were stained with hematoxylin and eosin for light microscopy.

Blocks of lung tissue (~1 cm^3) were sampled from non-dependent (ventral), middle and dependent (dorsal) regions of each lung before fixation. Wet-to-dry ratios were computed from weights before and after drying samples for 4 days at 80°C. (*12*)

REFERENCES

1. Musch G, Bellani G, Vidal Melo MF, et al. Relation between shunt, aeration, and perfusion in experimental acute lung injury. *Am J Respir Crit Care Med.* 2008;177:292-300.

2. Musch G, Venegas JG, Bellani G, et al. Regional gas exchange and cellular metabolic activity in ventilator-induced lung injury. *Anesthesiology.* 2007;106:723-735.

3. O'Neill K, Venegas JG, Richter T, et al. Modeling kinetics of infused 13NN-saline in acute lung injury. *J Appl Physiol.* 2003;95:2471-2484.

4. Vidal Melo MF, Layfield D, Harris RS, et al. Quantification of regional ventilation-perfusion ratios with PET. *J Nucl Med.* 2003;44:1982-1991.

5. Galletti GG, Venegas JG. Tracer kinetic model of regional pulmonary function using positron emission tomography. *J Appl Physiol.* 2002;93:1104-1114.

6. Schroeder T, Vidal Melo MF, Musch G, Harris RS, Venegas JG, Winkler T. Image-derived input function for assessment of 18F-FDG uptake by the inflamed lung. *J Nucl Med.* 2007;48:1889-1896.

7. Schroeder T, Vidal Melo MF, Musch G, Harris RS, Venegas JG, Winkler T. Modeling pulmonary kinetics of 2-deoxy-2-[18F]fluoro-D-glucose during acute lung injury. *Acad Radiol.* 2008;15:763-775.

8. Sokoloff L, Reivich M, Kennedy C, et al. The [14C]deoxyglucose method for the measurement of local cerebral glucose utilization: theory, procedure, and normal values in the conscious and anesthetized albino rat. *J Neurochem.* 1977;28:897-916.

9. Pearse DB, Brower RG, Adkinson NF, Jr., Sylvester JT. Spontaneous injury in isolated sheep lungs: role of perfusate leukocytes and platelets. *J Appl Physiol.* 1989;66:1287-1296.

10. Roselli RJ, Parker RE, Riddle WR, Pou NA. Fluid balance in sheep lungs before and after extracorporeal perfusion. *J Appl Physiol.* 1990;69:1518-1524.

11. Rozen S, Skaletsky H. Primer3 on the WWW for general users and for biologist programmers. *Methods Mol Biol.* 2000;132:365-386.

12. de Prost N, Dreyfuss D, Saumon G. Evaluation of two-way protein fluxes across the alveolo-capillary membrane by scintigraphy in rats: effect of lung inflation. *J Appl Physiol.* 2007;102:794-802.

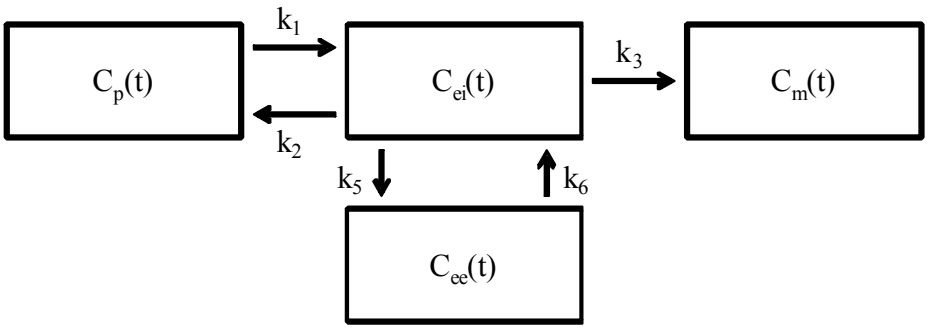

Supplemental Figure 1. Lung-specific four-compartment model for ^{18}F-FDG tracer kinetics (*7*). The four compartments of the model describe the activity concentration of ^{18}F-FDG in plasma ($C_p(t)$), the ROI concentration of extravascular ^{18}F-FDG serving as a substrate pool for hexokinase ($C_{ei}(t)$), the ROI concentration of ^{18}F-FDG in extravascular/noncellular compartment ($C_{ee}(t)$), and the ROI concentration of phosphorylated ^{18}F-FDG ($C_m(t)$). The arrows indicate the tracer exchange in the dynamic model and the corresponding parameters. The rate constants k_1 and k_2 account for forward and backward transport of ^{18}F-FDG between blood and tissue; k_3 is the rate of ^{18}F-FDG phosphorylation; k_5 and k_6 account for forward and backward transport of ^{18}F-FDG between substrate (intracellular) and nonsubstrate (extravascular/noncellular).

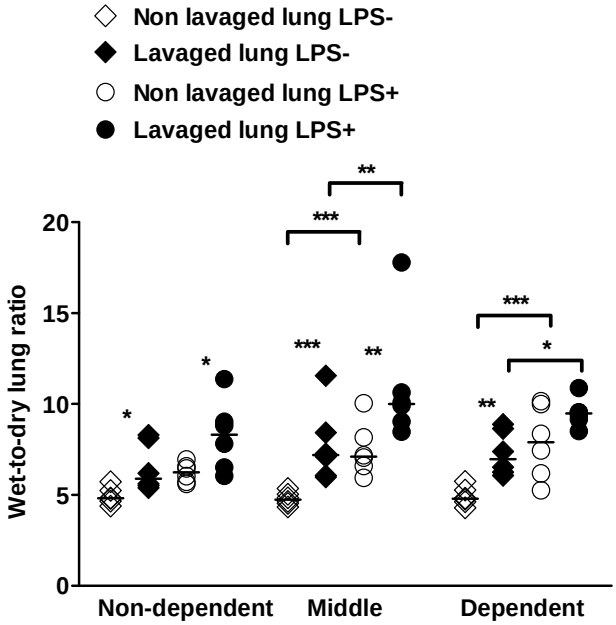

Supplemental Figure 2. Lung wet-to-dry ratios for dependent, middle and non-dependent regions of interest of lavaged (closed symbols) and non-lavaged (opened symbols) lungs of LPS- (diamonds) and LPS+ groups (circles), measured after 4 hours of mechanical ventilation. Horizontal lines represent median values. * P <0.05; ** P <0.01; *** P <0.001.

A

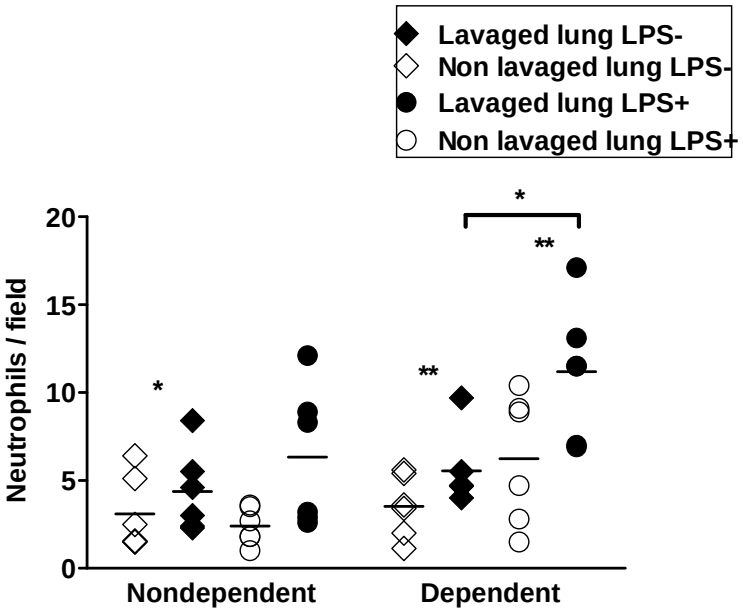
Lavaged lung LPS-
Non lavaged lung LPS-
Lavaged lung LPS+
Non lavaged lung LPS+
Neutrophils / field
20
15
10
5
0
*
**
*
**
Nondependent
Dependent

B

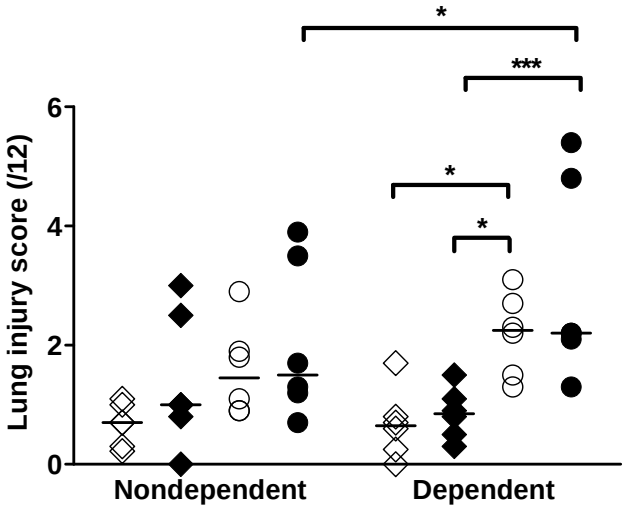
Lung injury score (/12)
6
4
2
0
*
***
*
*
Nondependent
Dependent

Supplemental Figure 3. Lung neutrophil counts (A) and lung injury score (B) in dependent and non-dependent regions of lavaged (closed symbols) and non-lavaged (opened symbols) lungs of LPS- (diamonds) and LPS+ groups (circles). There was an overall effect of vertical height on lung neutrophil counts (P <0.001). Lung injury score was significantly affected by LPS administration (P=0.06 in lavaged and P<0.01 in non-lavaged lungs), but not by alveolar lavage (P=0.34). Dependent regions of both lungs of the LPS+ group exhibited higher scores than those of the LPS- group. Horizontal lines represent median values. * P <0.05; *** P <0.01.

	Lavage	LPS	Interaction
TNF-α	0.040	<0.01	0.041
IL-1β	0.17	<0.01	0.29
IL-6	0.29	<0.01	0.38
IL-8	0.09	<0.01	0.11
IL-10	0.93	<0.01	0.70

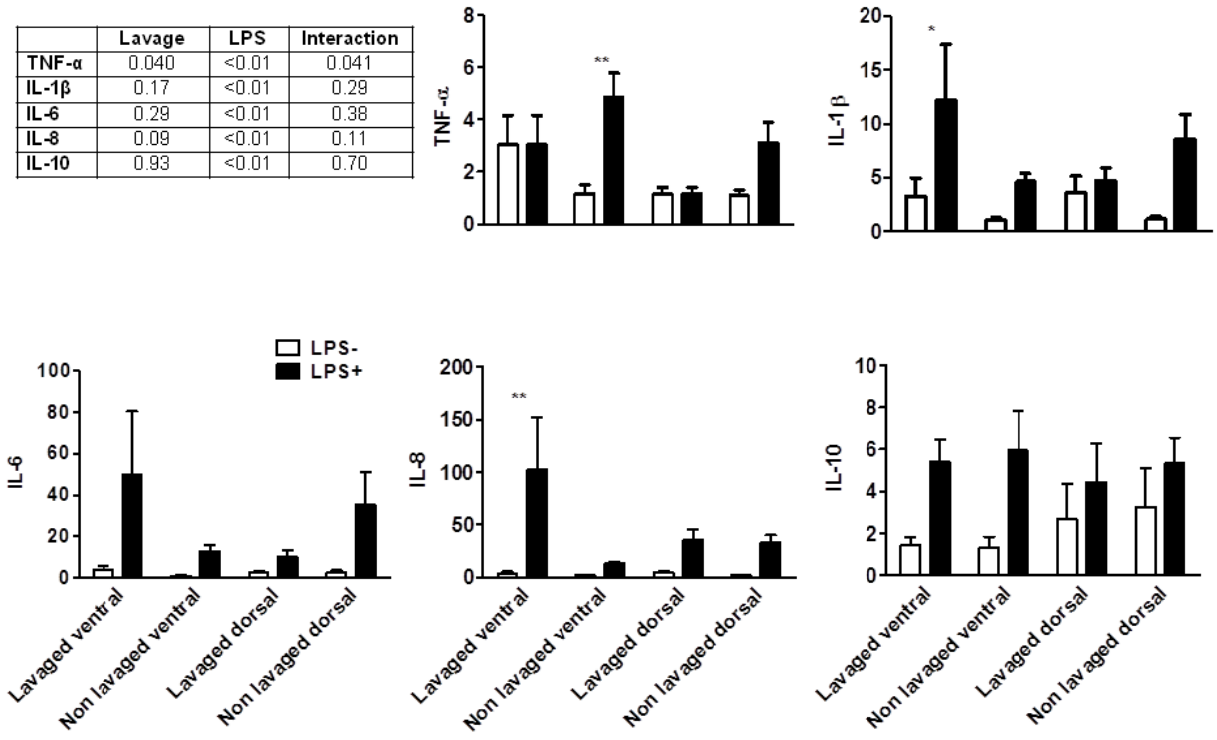

Supplemental Figure 4. Regional lung expression of TNF-α, IL-1β, IL-6, IL-8, and IL-10 in LPS- (open bars) and LPS+ (closed bars) groups. Table shows the P values of two-ways ANOVA, for the global effects of alveolar lavage (lavage), LPS administration (LPS), and their interaction. There was an effect of LPS administration on the expression of all cytokines. In contrast, alveolar lavage only affected the expression of TNF-α. Cytokines are expressed in fold changes. Histograms show mean values±SEM; * P <0.05; ** P <0.01.

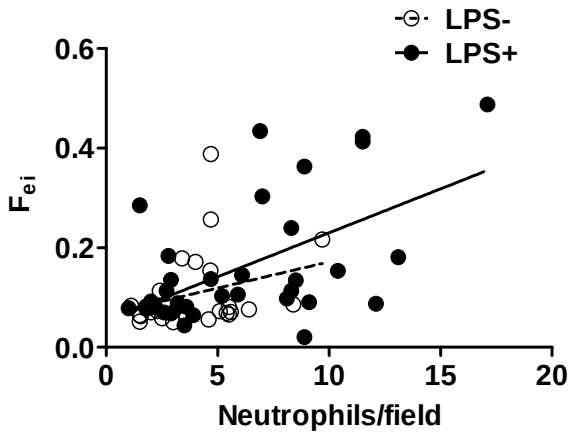

Supplemental Figure 5. Linear regression between regional lung neutrophil counts and regional F_{ei} for LPS- (open circles) and LPS+ (closed circles) groups. The intracellular distribution volume of ^{18}F-FDG (F_{ei}) correlated significantly with the number of lung neutrophils in the LPS+ ($y=0.0176x + 0.0532$; $R^2=0.31$, $P<0.001$; continuous line) but not in the LPS- ($y=0105x + 0.0657$; $R^2=0.08$, $P=0.18$; dashed line) group.

	LPS-		LPS+	
	R^2	P	R^2	P
TNF-α	0.02	0.45	0.01	0.58
IL-1β	0.01	0.65	0.14	0.026
IL-6	0.01	0.80	0.04	0.22
IL-8	0.01	0.93	0.18	0.011
IL-10	0.07	0.14	0.14	0.023

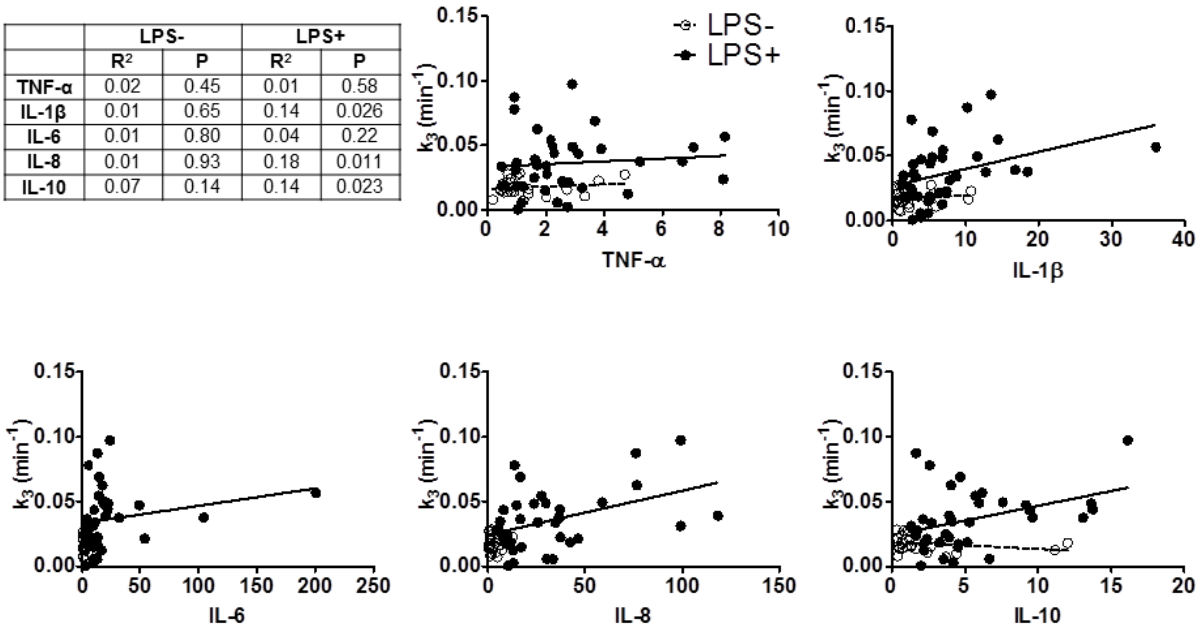

Supplemental Figure 6. Linear regression between regional lung expression of cytokines (TNF-α, IL-1β, IL-6, IL-8, and IL-10) and regional phosphorylation rate k_3 for LPS- and LPS+ groups. Table shows the coefficients of determination (R^2) and P-values for the correlation between k_3 and regionally measured cytokines. k_3 was significantly correlated with IL-1β, IL-8, and IL-10 in the LPS+ (continuous lines) but not in the LPS- (dashed lines) group. The correlation between k_3 and IL-1β was still significant after removing the outlier point (R^2=0.15; *P*=0.019).

Supplemental Table 1

Primers for ovine cytokines and housekeeping genes

Gene name	Sequence (5′–3′)	Length (bp)[a]
GAPDH		
Forward	ATCACTGCCACCCAGAAGACT	153
Reverse	CATGCCAGTGAGCTTCCCGTT	
TNFα		
Forward	CTTCAACAGGCCTCTGGTTC	133
Reverse	GAGGGCATTGGCATATGAGT	
IL-1β		
Forward	CGAACATGTCTTCCGTGATG	143
Reverse	TCTCTGTCCTGGAGTTTGCAT	
IL-6		
Forward	CGTCGACAAAATCTCTGCAA	124
Reverse	GCATCCATCTTTTTCCTCCA	
IL-8		
Forward	TGCTCTCTGCAGCTCTGTGT	154
Reverse	TCTGAATTTTCGCAGTGTGG	
IL-10		
Forward	TGCTGTTGACCCAGTCTCTG	139
Reverse	TTCACGTGCTCCTTGATGTC	

IL – interleukin; TNFα – tumor necrosis factor alpha; GAPDH – glyceraldehyde-3-phosphate dehydrogenase; TLR4 – Toll-like receptor 4.

[a] Amplicon length in base pairs.